

The Effect of Fe Additive on Plastic Deformation of Crush-Boxes with Closed-Cell Metal Foams, Part II: Al-Composite Foam-Filled brass tubes Compression Response

S.M.H. Mirbagheri* and J. Khajehali

Department of Mining and Metallurgical engineering, Amirkabir University of Technology, Tehran, Iran

Abstract: The brass tubes with foam cores of AlSi7SiC3, AlSi7SiC3Fe1 and AlSi7SiC3Fe3 were produced as the crush-boxes with circle and square cross-section. Then axial compressive behavior and energy absorption capability of the foam-filled tubes were investigated during the quasi-static progressive plastic buckling. The uniaxial compressive stress-strain curves of the foam-filled brass tubes exhibited that the compressive stress enhanced smoothly with the increase of the strain and no stress oscillations occurred in the plastic deformation region throughout the tests. The yield stress and the elastic modulus of the foam-filled brass tubes slightly decreased with the increase of Fe wt. % in the foam cores. Moreover, with the increase of Fe powder from 1wt. % to 3wt. %, the absorption energy of the foam-filled brass tubes decreased slightly dependent on the tubes cross-section. The strain-hardening exponent of the tubes with the Al7Si-3SiC-(+Fe) foam cores were found to be lower than the tubes with the Al7Si-3SiC foam cores without Fe. However, the increase of Fe powder from 1wt. % to 3wt. % caused the approximate elimination of strain-hardening and the plastic deformation behavior tends to be approximated to an ideal-plastic behavior up to the densification strain. The results indicate that all of the compression responses are due to the Micro and Macro-defects within the foams cellular structure as well as the tubes cross-section geometry.

Keywords: Metal foam, Composite, Brass tube, Plastic buckling, Compression response, Absorption energy, Intermetallic compound, Foam-filled tubes

1. Introduction

Aluminum closed-cell foams have developed in variety of industries, due to their unique combination of mechanical and physical properties [1–3]. They demonstrate a distinct and high energy absorption capacity during compression test under uniaxial loading [3]. In auto industry, thin-walled tubular structures have been applied as energy absorbers or crush-boxes because of their progressive plastic buckling under uniaxial compressive loading. The crush of the thin-walled tubes is dependent on thickness, size, shape of cross-section, and material of tubes [3-4]. In recent decades, engineers have attempted to replace the empty space into the thin-walled tubes by the metal foam cores. The result of replacing indicated that foam-filled tubes stabilize the irregular plastic buckling pattern that led to the improvement of energy absorption up to 30% [4-6]. In fact, the metal foam provides internal support for the tube thin wall so that it causes to create more plastic hinges per unit length of tube. Therefore, the absorption energy during progressive plastic buckling under uniaxial quasi statics will be increased [5, 7]. Studies done by Langseth et al., show that plateau stress for the metal foam-filled tubes is higher than the algebraic summation of plateau stress of the empty tube and the metal foam itself. Moreover, area under their stress-strain curves of the foam-filled tubes approximately illustrated an increase of 30-40% with respect to the empty tubes [7-

8]. A nominal compressive stress-strain curves of the foam-filled tube has three regions including: i) elastic deformation, ii) soft plastic deformation together with cells crushing at long plateau stress up to densification strain, iii) hard plastic deformation after densification strain or bulk deformation with ultra strain-hardening rate. However, the curve of the soft plastic deformation (long plateau stress) region has different pattern such as exponential, power law, linear, wave oscillations, and mix of them [6, 8]. It is possible that the wave oscillations of the plateau stress eliminated by changing the composition and the cellular structure of metal foam cores. It has been reported that the presence of ceramic particles and chemical elements in the foam liquid leads to become brittleness, helps to create the wave oscillation and the strain-hardening in the region (ii) of the compressive stress-strain curve [9]. In this case, there are a lot of papers about mechanical properties and absorption energy of Al foam, Al- alloys foam, and Al composites foam as filler of thin-walled steel tubes [4-5, 9]. Quality of the Al composite foams has significant influence on the pattern of the elastic and the plastic deformation of the foams and Al composite foam filled tubes [10-11]. Results show the interaction between the tubes and the filler metal foam, which leads to higher energy dissipation and changed progressive plastic buckling modes. Experiments present that the buckling process of thin-walled tubes is accompanied by progress of localized plastic mechanisms and some folds are appeared on the wall of tubes. Therefore, the numerical analysis and computer simulation of the filled thin-walled tubes is very complicated. However, some papers that simplified mechanisms were proposed to predict and modeled the buckling response of the filled tubes for simple shape (circular and square) under variety loading conditions. The simplified models lead to simple solution and therefore, can be used efficiently in preliminary design of energy absorbing systems [3, 5, 11]. However, such models are limited to aluminum and steel tubes and they are not a model or report for the brass tubes.

Therefore, in this investigation as the second part of the paper with reference number [12], attempt has been made to evaluate the effect of the AlSi7SiC3(Fe) foams as filler of thin-walled brass tubes and its cross-sectional shape on the behavior of progressive plastic buckling, under the condition of quasi-static uniaxial compression load.

2. Experimental procedures

In order to investigate the mechanical properties of energy absorber elements during plastic deformation, three types of tubes with foam cores, namely AlSi7SiC3, AlSi7SiC3Fe1, and AlSi7SiC3Fe3 with 25-32 PPI, were prepared based on a method that have been mentioned in Part-I [12]. Two types including circle and square tubular moulds with the thickness of 1 mm, and outside diameters of 22 mm and square cross-section of 22x22 mm were cut with the height of 1.5 times of their diameters from 70Cu-30Zn brass tubes, respectively. The uniaxial quasi static loading on the foam-filled tubes were then performed using 25 kN Instron 8502 test machine at a crosshead speed of 2.5 mm/minute and 1.3×10^{-3} (1/sec) strain rate at room temperature. The curves of force-displacement were plotted then for all the Foam-Filled Tubes (FFT). In order to identify the samples, they were coded as "FFT-Z-X-Y" and "ET-Z-X-Y". Each code includes three parts: "Z", "X" and "Y". The letter "Z" refers to geometry of moulds (S=square, C=circle) and the letter "X" refers to diameter of foam cross-section as a millimeter, and "Y" indicates weight percent of the Fe powder in foams (Y= 0% or 1% or 3%). The letters "ET" and "FFT" refer to the empty tubes and the foam-filled tubes, respectively. Figure 1 shows all square and circle tubes that have been filled by foam cores based on the above coding.

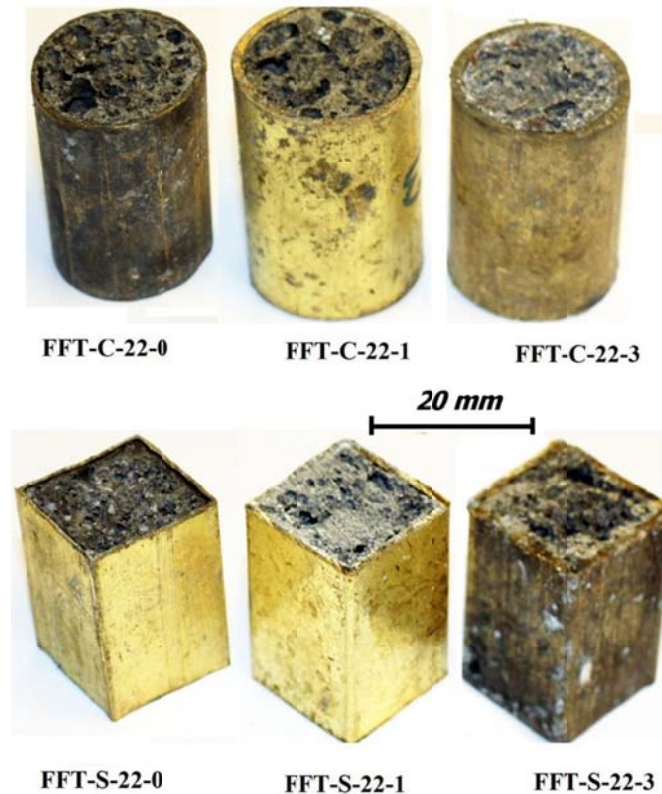


Fig. 1. Foam-filled Cu-30Zn brass tubes before compression test. Top: circle section, Bottom: square section.

3. Results and discussions

3.1. Compression response

Figure 2 shows the effect of Fe wt. % on the force-displacement and the stress-strain curves of the AlSi9SiC3 composite foams filled-tubes with circular and square cross-section, respectively. Also, compressive response of the empty brass tubes was presented for comparison in Fig. 2. Results indicated that alike the compressive stress-strain curves of other Al foam-filled tubes, it had three distinct stages [2-4, 13-14]. First the elastic strain zone, which the stress linearly increases with increasing of the strain. Then a long plateau of plastic deformation at an approximately smooth stress occurs, which lead to a progressive plastic buckling associated with crushing of cellular structure of the foam core and also the tube folding. Finally, there is a densification strain region in association with abrupt increase in stress, because the rate of work-hardening is limited either by the densification of the foam cores or its contact between the adjacent folds of the tube walls. It is observed in Fig. 2 that both the square and the circular tubes with foam cores and without containing any Fe element, namely FFT-S-22-0 and FFT-C-22-0 have more resistance during plastic deformation in comparison with the foam cores with Fe. Furthermore, for tubes with circle cross-section, the strain-stress curves through the plastic strains are less than the tubes with the square cross-section. In other words, it can be deduced that the presence of Fe element in the Al foam cores had not significantly affected on the compression stress-strain response at the elastic region. However, in the plastic region, the addition of Fe on the work-hardening phenomenon and the plateau stress for all the foam-filled tubes had considerable impact. It seems that brittleness of composite foam cores containing Fe is due to dispersion of the intermetallic compounds within foam cells walls such as $\alpha+\beta$ phases for wt. % Fe < 2 or $\alpha+\delta$ phases for wt. % Fe > 2 [12]. Therefore, the behavior of strain-hardening exponent for all samples, during plateau plastic deformation, can be noted and analyzed. The

flow stress of a material is generally expressed as a function of plastic strain by $\sigma = K \epsilon^n$ equation, where "n" is the strain-hardening exponent, and "k" is the plastic strength coefficient [15-17]. Figure 3 shows the variation of $\ln(\sigma)$ with $\ln(\epsilon)$ for all the composite foam filled-tubes at the plastic deformation regions after the elimination of the elastic region based on the presented idea in reference [17].

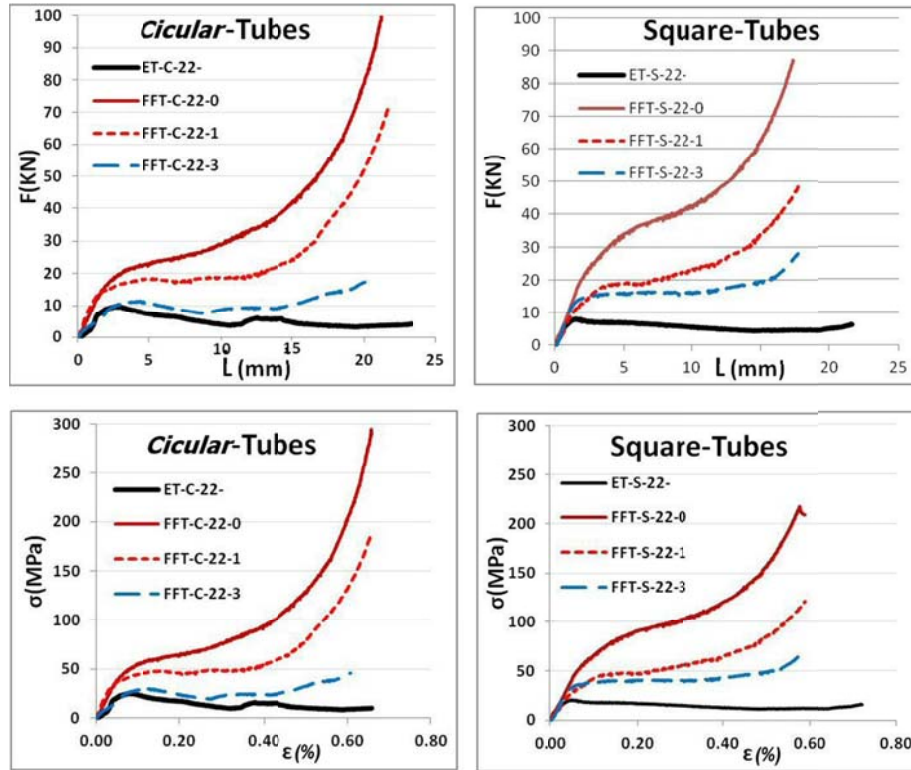


Fig. 2. Compression response of the foam-filled tubes during the uniaxial and quasi static progressive plastic buckling. Top row: Force-displacement curves, Bottom row: Stress-strain curves, Left column: Circle tube, Right column: Square tubes.

Two strain-hardening mechanisms can be noted for all foam-filled tubes in Fig. 3. The first mechanism belongs to the low strain-hardening exponent "n1", before the densification strain or soft plastic deformation and the second mechanism for strains after the densification strain with strain-hardening exponent "n2" or hard plastic deformation. The strain-hardening exponents (n) and the plastic strength coefficients (k) for all the foam-filled tubes have been presented in Table 1.

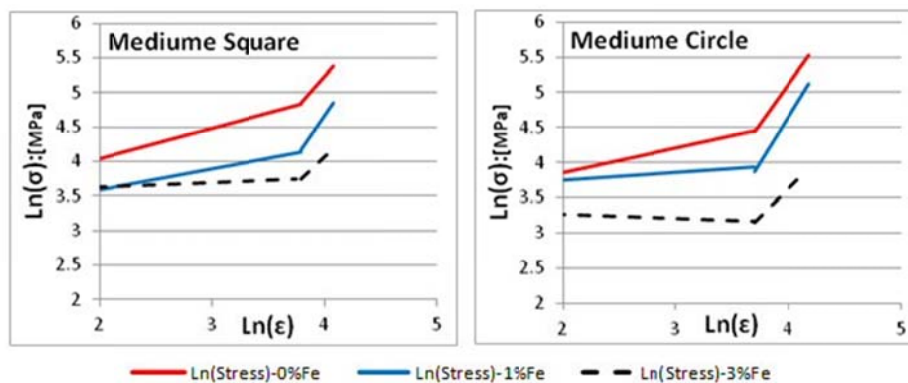


Fig. 3. Plot of $\ln(\sigma)$ versus $\ln(\epsilon)$ for plastic deformation zone, obtained from curves of Fig. 2.

Table 1. Determine the "n" and "k" coefficients of strain-hardening equation for all samples in Fig. 3, based on procedure mentioned in Ref. [12]

| sample code | Equation for (n1) | Equation for (n2) | n1 | n2 | k1 | k2 | lines intersection | |
|-------------|--|---|------|-----|------|------|--------------------|-------|
| | | | | | | | ln(ε) | ln(σ) |
| FFT-C-22-0 | $\ln(\sigma) = 0.36 \ln(\epsilon) + 3.136$ | $\ln(\sigma) = 2.25 \ln(\epsilon) - 3.88$ | 0.4 | 2.2 | 3.1 | -3.9 | 3.7 | 4.5 |
| FFT-S-22-0 | $\ln(\sigma) = 0.44 \ln(\epsilon) + 3.15$ | $\ln(\sigma) = 1.86 \ln(\epsilon) - 2.22$ | 0.4 | 1.9 | 3.2 | -2.2 | 3.8 | 4.8 |
| FFT-C-22-1 | $\ln(\sigma) = 0.11 \ln(\epsilon) + 3.52$ | $\ln(\sigma) = 2.58 \ln(\epsilon) - 5.68$ | 0.1 | 2.6 | 3.5 | -5.7 | 3.7 | 3.9 |
| FFT-S-22-1 | $\ln(\sigma) = 0.31 \ln(\epsilon) + 2.97$ | $\ln(\sigma) = 2.42 \ln(\epsilon) - 5.01$ | 0.3 | 2.4 | 3.0 | -5.0 | 3.8 | 4.1 |
| FFT-C-22-3 | $\ln(\sigma) = -0.06 \ln(\epsilon) + 3.39$ | $\ln(\sigma) = 1.58 \ln(\epsilon) - 2.70$ | -0.1 | 1.6 | -3.4 | -2.7 | 3.7 | 3.2 |
| FFT-S-22-3 | $\ln(\sigma) = 0.073 \ln(\epsilon) + 3.46$ | $\ln(\sigma) = 1.55 \ln(\epsilon) - 2.16$ | 0.1 | 1.6 | 3.5 | -2.2 | 3.8 | 3.7 |

It can be observed from Table 1 that the addition of Fe element significantly affects the strain-hardening exponent of the foam-filled tubes. The strain-hardening exponent of the AlSi9SiC3Fe3 foam-filled tubes is lower than the AlSi9SiC3 foam-filled tubes for both the square and the circle cross-section. Therefore, coefficient varieties of "n1" and "k1" from equation $\sigma = K \epsilon^n$ were plotted up to the strain densification (soft deformation) for both the square and the circle tubes with foam cores in Fig. 4. In Fig. 4, for the foam-filled tubes, the increase of Fe powder from 1 to 3wt. % causes a decrease in the strain hardening exponent "n1" from 0.4 toward 0.1 and then to -0.1 for the circle tubes, and also from 0.4 toward 0.3 and then to 0.1 for the square tubes. However, coefficients of k1 are approximately constant (3.2 ± 0.25) for the square tubes in spite of the circle tubes. It seems that varieties of "n1" and "k1" for the square tubes are more reliable than the circle tubes for different foam cores. Because the negative coefficient of "n1=-0.1" for FFT-C-22-3 sample indicates a structural defect in the foam core to exist. Whereas, the square tubes have a constant plastic strength coefficient "k" and their strain-hardening exponent "n" decrease with the increase of Fe element (see Fig. 4). Therefore, the addition of Fe within the AlSi9SiC3 foam core can change positive slope of the strain-stress to a slope of approximately zero in plastic deformation region. In other words, there is a horizontal line on the stress-strain curves during the densification strain individually for the square tubes with 3wt. % Fe (i.e. n1=0.4 toward n1=0.1).

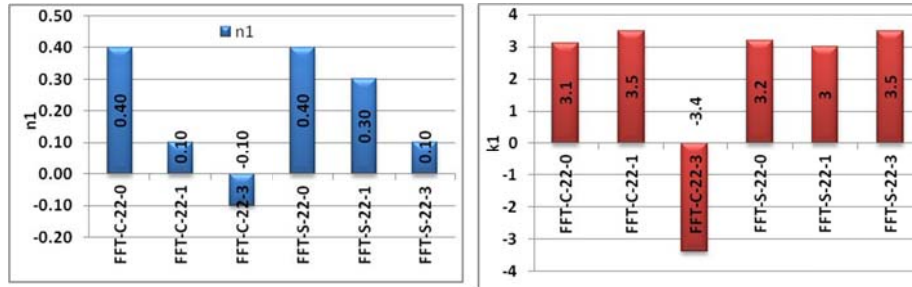


Fig. 4. Varieties of the plastic strength coefficient "k" and the strain-hardening exponent "n" for the foam-filled tubes with foam cores including Fe.

3.2. Mechanical properties of foam-filled tubes

Figure 5, 6, and 7 show the effect of Fe additive on yield stress (σ_{max}), elastic modulus (E), and energy absorption capacity (w) of the foam-filled tubes, respectively. Figure 5 shows yield stress (σ) and characteristic yield stress (σ_{max}/ρ) for the foam-filled tubes in order to facilitate comparison. These data were extracted from the elastic zone of Fig. 2. It is observed that both the yield stresses and the characteristic yield stress decreases significantly with the increase of Fe element, especially for tubes with square cross-section. The variation of the elastic modulus (E) and the characteristic modulus (E/ρ) for the composite foams filled-tubes as a function of the wt. % Fe was plotted in Fig. 6. Results demonstrate a strange behavior for modulus. This is because the elastic modulus of the square cross-section tubes, at first decrease and then increase in spite of samples with circle cross-section. However, these variations are not noticeable. It seems this behavior depends on reaction between the Fe-reach intermetallic within the foam cores and the shape of the tube cross section on solidification rate of the foam core during the production.

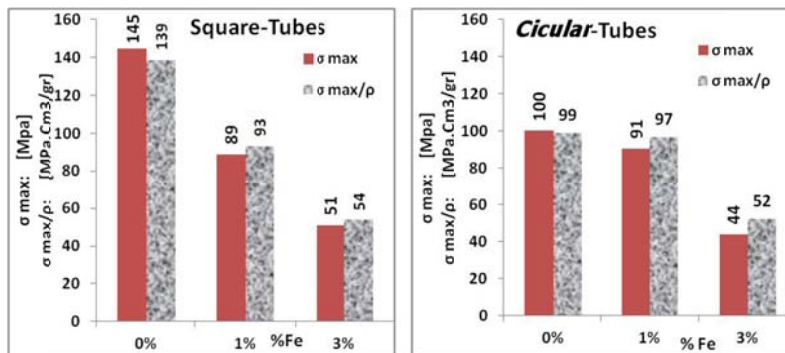


Fig. 5. Yield stress and characteristic stress yield obtained from curves of Fig.2 during the plastic buckling of foam-filled tubes under uniaxial loading. Left: Square tubes. Right: Circle tubes.

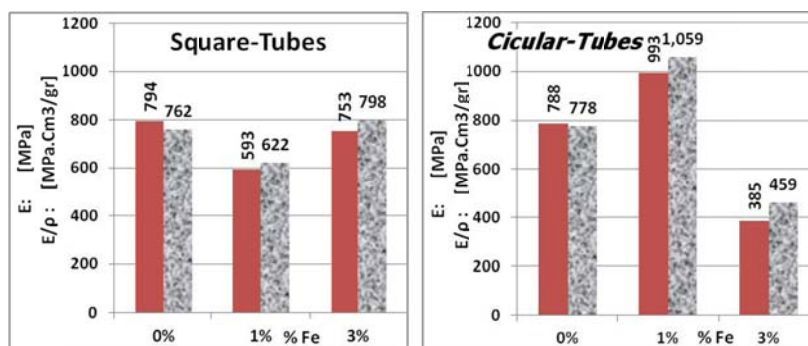


Fig. 6. Modulus and the characteristic modulus obtained from curves of Fig.2 during plastic buckling of foam-filled tubes under uniaxial loading. Left: Square. Right Circle.

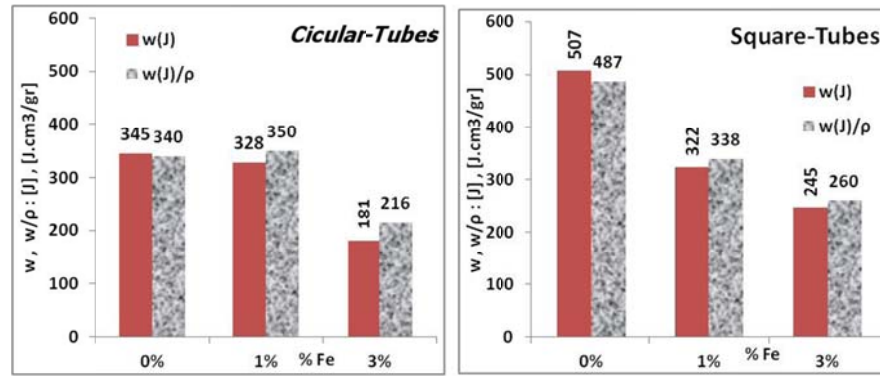


Fig. 7. Absorption energy and characteristic absorption energy obtained from curves of Fig. 2 during progressive plastic buckling of foam-filled tubes under uniaxial loading.
Left: Circle Tubes. Right: Square tubes.

In Fig. 7, the absorbed energy during the progressive plastic buckling of composite foam-filled tubes is illustrated. W , calculated from Eq. (1) [3, 16]:

$$W = \int_{\varepsilon_0}^{\varepsilon_d} \sigma(\varepsilon) . d\varepsilon \quad (1)$$

where, lower limit of integration (ε_0) is the end of the elastic strain. The upper limit of integration (ε_d) is the densification strain and it is determined from intersection of the lines in Fig. 3, which were extracted and presented at last column of Table 1. The absorbed energy (w) and the characteristic absorbed energy (w/ρ) of the composite foams are plotted as a function of wt. % Fe for comparison in Fig. 7. Results show that the energy absorbing capacity for tubes with the square cross-sections are more than the tubes with circle cross sections. However, for both square and circle section, the characteristic absorption energies are slightly higher than the normal absorption energy. It can be noted from Fig. 7, the energy absorption of the AlSi7SiC3Fe1 foam-filled tubes are more than the AlSi7SiC3Fe3 samples, individually for square tubes with the FFT-S-22-1 and the FFT-S-22-3 codes. This can be attributed for two reasons: i) the higher yield and longer densification strain (ε_d) of these foams (see Fig. 2), and ii) the higher strain-hardening exponent of these foams in Fig. 3 and Table 1.

Figure 8 shows absorption energy values of the empty tube and the all foam filled-tubes for comparison. It is observed that both tubes of the FFT-C-22-0 and the FFT-S-22-0 have higher absorption energy value (between 2-3 times) in comparison to both the empty tubes, which is due to cellular structure of the composite foam cores without Fe element. However, the empty tubes, namely ET-S-22- and ET-C-22-, did not present a good progressive plastic buckling at Fig. 9 (i.e. no higher symmetric and number fold) in spite of the FFT-C-22-0 and FFT-S-22-0 tubes. The apparent comparison of the FFT-C-22-0 and the FFT-S-22-0 tubes with samples of the ET-S-22- and the ET-C-22-, after uniaxial compressive loading at Fig. 9, proved this claim. However, for the composite foam cores containing of the Fe element, tubes of the FFT-C-22-1, the FFT-S-22-1, and the FFT-C-22-3, the FFT-S-22-3 have presented a better progressive plastic buckling behavior in spite of their lower absorption energy. This is because the AlSi7SiC3Fe1 foam cores within tubes give an internal support for tubes wall, shortening the wavelength buckles and thus creating more plastic folds per unit length. However, the AlSi7SiC3Fe3 foam cores show lower absorption energy in comparison with the AlSi7SiC3Fe1 foam cores. Thus, both the square and the circle tubes have better absorption energy when they are filled with the AlSi7SiC3Fe1 foam cores in spite of their higher strain-hardening exponent relative to the AlSi7SiC3Fe3 foam cores (Fig. 4).

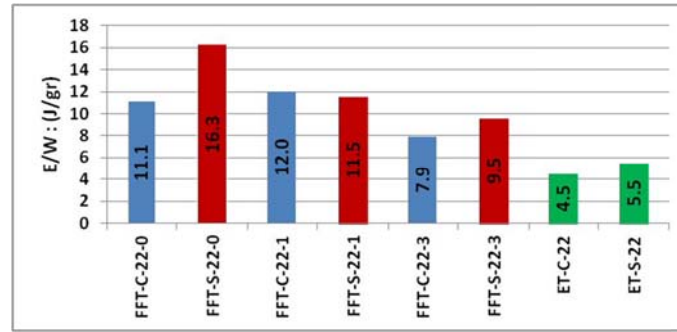


Fig. 8. Comparison of absorption energy among all thin-walled brass tubes.



Fig. 9. Behavior of progressive plastic buckling foam-filled brass tubes with circle and square cross-section after uniaxial compressive loading.

Therefore, the cooling rate could change the microstructures of cell walls in AlSi7SiC3(Fe) composite filled-tubes. At low cooling rates, the wall contains $(\alpha+\beta)$ for wt. % Fe < 2 while a combination of $(\alpha+\delta)$ phases for wt. % Fe > 2 is formed under high cooling [12]. Also an additional energy is absorbed at AlSi7SiC3Fe1 samples due to the presence of the concentration of stress around the intermetallic within the cell-wall or around the micro-void within the cells-plateau region. Based on the above results, it can be deduced that foam filled-tubes with 1 wt. % Fe for both the circle and the square cross-sections have a good progressive plastic buckling due to suitable distribution of plastic hinge points at the tubes wall, which can rise energy absorption and increase the hardening-strain exponent in spite of the samples containing 3 wt. %Fe.

4. Conclusion

- i) The foam filled brass tubes during the compressive loading increase the absorption energy more than 1.2 to 3 times relative to the empty brass tubes. This increasing factor depends on the properties of the foam core and the characteristic of the thin-walled tubes. More importantly, the characteristics of the thin-walled tubes are their cross-sectional shape and their size.
- ii) Cellular structure and Micro-structure of composite foams had a significant role on the behavior of progressive plastic buckling of the foam-filled brass tubes, especially for folds numbers per the tube length.

- iii) During the AlSi7SiC3(Fe) foaming process by powder metallurgy route, some intermetallic such as $\alpha+\beta$ and $\alpha+\delta$ formed dependent on the cooling rate and the percentage of Fe, which can strongly affect on mechanism of the plastic hinge formation.
- iv) The Fe additive in the composite foams affected on the strain-hardening exponent of the foam-filled tubes so that the foam with 3 wt. % Fe, the strain-hardening can be approximately eliminated, individually for the square cross-sectional tubes because the strain-hardening exponent for tube with AlSi7SiC3 foam core reduced from $n=0.4$ toward $n=0.1$ for AlSi7SiC3Fe3.
- v) All foam-filled brass tubes revealed the work-hardening phenomenon during the uniaxial compression loading; however additional 3wt. % Fe within the foam core can eliminate the work-hardening.

5. References

- [1] J. Baumeister, J. Banhart and M. Weber, *Materials and Design*, 18 (1997) 217–220.
- [2] T. Mukai, T. Miyoshi, S. Nakano, H. Somekawa and K. Higashi, *Scripta Materialia*, 54 (2006) 533–537.
- [3] A.G. Evans, M.F. Ashby, N.A. Fleck, L.J. Gibson, J.W. Hutchinson and H.N.G. Wadley, *Metal Foams: A Design Guide*, (2000), Elsevier.
- [4] M. Seitzberger, F.G. Rammerstorfer, R. Gradinger, H.P. Degischer, M. Blaimschein and C. Walch, Experimental studies on the quasi-static axial crushing of steel columns filled with aluminum foam, *Int. J. Sol. Struct.* 37(2000) 4125-4147.
- [5] M. Seitzberger, F.G. Rammerstorfer, H.P. Degischer and R. Gradinger, Crushing of axially compressed steel tubes filled with aluminum foam, *Acta Mech.* 125(1997) 93-105.
- [6] T. Daxner, H.J. Böhm, M. Seitzberger and F.G. Rammerstorfer, Modeling of Cellular Materials, Handbook of Cellular Metals. 2002: (Eds.:H.P.Degischer, B.Kriszt), pp. 245-280; Wiley-VCH, Weinheim, Germany.
- [7] M. Langseth, O.S. Hopperstad and A.G. Hanssen, Crash behavior of thin-walled aluminum members, *Thin-Walled Structures*, 32(1998) 127–150.
- [8] M. Langseth A.G. Hanssen and O.S. Hopperstad, Optimum design for energy absorption of square aluminum columns with aluminum foam filler. *International Journal of Mechanical Sciences*, 43 (2001) 153-176.
- [9] A. Bastawros, H. Bart-Smith and A.G. Evans, Experimental analysis of deformation mechanisms in a closed-cell aluminum alloy foam, *Journal of the Mechanics and Physics of Solids*, 48(2000) 301-322.
- [10] A.K. Toksoy and M. Guden, Partial A: Foam filling of commercial 1050H14 crash boxes: the effect box column thickness and foam relative density on energy absorption, *Thin-walled structures* 48(2010) 482-494.
- [11] W. Yan, E. Durif, Y. Yamada and C. Wen, Crushing Simulation of Foam-Filled Aluminum Tubes, *Materials Transactions*, 48-7 (2007) 1901-1906.
- [12] S.M.H. Mirbagheri and J. Khajehali, The effect of Fe additive on plastic deformation for crush-boxes with closed-cell metal foams, Part I: Al-composite foam compression response, *Iranian Journal of Materials Forming*, 1-1(2014) 32-45.
- [13] W. Deqing and S. Ziyuan, Effect of ceramic particles on cell size and wall thickness of aluminum foam. *Materials Science and Engineering A*, 361(2003) 45–49.
- [14] J. Banhart, Manufacture, characterization and application of cellular metals and metal foams, *Progress in Materials Science*, 46(2001) 559-632.
- [15] Mondal, M.D. Goel and S. Das, Effect of strain rate and relative density on compressive deformation behavior of closed cell aluminum-fly ash composite foam, *Materials & Design*, 30 (2009) 1268-1274.
- [16] M. J. Khajehali, Compressive response of the composite metallic foam filled-tubes and effective parameters, *M.Sc. Thesis, Amirkabir University*, 2011.
- [17] A. Daoud, Compressive response and energy absorption of foamed A359–Al₂O₃ particle composites, *Journal of Alloys and Compounds*, 486 (2009) 597–605.